A CONDUCTANCE PROBE FOR MEASURING LIQUID FRACTION IN PIPES AND PACKED BEDS

N. A. Tsochatzidis, T. D. Karapantsios, M. V. Kostoglou
and A. J. Karabelas†

Chemical Process Engineering Research Institute and Department of Chemical Engineering,
Aristotle University of Thessaloniki, Univ. Box 455, 540 06 Thessaloniki, Greece

Abstract—The performance of ring electrodes measuring the conductance of gas–liquid mixtures in pipes and packed beds is studied experimentally and theoretically. With relatively closely spaced pairs of rings, one can detect liquid *segregation*, i.e. stratified and annular distribution, as well as a *uniform* liquid distribution if the mean liquid fraction is available. Conversely, reliable cross-sectionally-averaged holdup data can be obtained if the liquid distribution pattern is known. Measurements in packed beds and pipes are qualitatively very similar. Existing theoretical expressions are employed to interpret the conductance measurements. Moreover, a new analytical solution for an annular liquid distribution is presented, which is particularly helpful in assessing the spatial probe sensitivity in the axial direction. The latter is found to be quite satisfactory. In general, agreement between the data and theoretical predictions is fair to excellent, providing the necessary confidence for practical applications. Two successful applications of the technique to packed beds are reported.

Key Words: conductance probe, gas–liquid mixture, packed bed, holdup, two-phase flow

INTRODUCTION

Determination of liquid holdup is of great importance in a variety of engineering applications involving two- and three-phase systems. The most common technique for determining holdup relies on measurements of electrical impedance between two electrodes, of various configurations, in contact with the fluid. The major advantages of this technique are the simplicity of application and the relatively low cost of the equipment involved. A comprehensive review of the method, as applied to two-phase gas–liquid flows, was presented by Hewitt (1978), wherein all pertinent literature until about 1977 was surveyed.

In experiments to determine *cross-sectionally-averaged* holdup values in closed systems (pipes, columns etc.) one is usually concerned about the sensitivity of the technique to the complex two-phase flow patterns. To overcome such difficulties, Merilo *et al.* (1977) employed a conductance gauge consisting of six electrodes flush mounted onto the channel wall. Pairs of these electrodes (opposite each other) are successively energized by "rotating" the electric field. Averaging the resulting probe signals provides a measure of the holdup in the cross-section. The same type of gauges were used by Delhaye *et al.* (1987) and Saiz-Jabardo & Bouré (1989) in their studies of vertical bubble and slug flow. Matuszkiewicz *et al.* (1987) employed two square electrodes flush mounted on two opposite walls of a square test section.

Ring-type electrodes, covering the entire circumference, are quite convenient for measurements in pipes and columns of circular cross-section. Asali *et al.* (1985) were the first to employ a pair of parallel ring electrodes for measuring the average liquid film thickness in vertical annular flow. For such thin films, the behavior of ring probes is very well described by a theory developed by Coney (1973) for a pair of parallel electrodes mounted flush on a *flat* wall. Andreussi *et al.* (1988) presented a novel test-section design and further developed ring probes for measuring liquid holdup in pipes under various flow conditions. Some aspects of their work—relevant to this study—are discussed in the following sections. The probe configuration developed by Andreussi *et al.* (1988) was also adopted in recent studies of horizontal and inclined gas–liquid pipe flows (Andreussi & Bendiksen 1989; Nydal & Andreussi 1991; Beckmann & Mewes 1991).

---

†To whom correspondence should be addressed.

Electrical impedance techniques have been also employed in two- and three-phase systems involving solid particles. For example, Nasr-El-Din *et al.* (1987) and Chase *et al.* (1990) have conducted experiments in slurry systems, whereas Turner (1976) and Begovich & Watson (1978) have carried out measurements in two- and three-phase fluidized beds, respectively. In the case of two-phase flow through packed beds, which is of particular interest to this work, measurements with conductance probes were performed in some early studies (Beimesh & Kessler 1971; Prost 1967). These measurements, taken with relatively small electrodes located in specific radial positions in the packing, rendered local holdup values, not necessarily representative of the cross-sectional average. To overcome such problems Drinkenburg and co-workers (Blok & Drinkenburg 1982; Blok *et al.* 1983; Rao & Drinkenburg 1983) placed two parallel screens, covering the entire packed bed cross-section, at an axial distance from each other. Self-consistent conductance measurements under various gas–liquid flow conditions were made. However, the extent to which the screens influenced the packing arrangement and, consequently, the flow itself was not evaluated.

The scope of this work is to explore the use of the ring probe configuration for measurements of the instantaneous, cross-sectionally-averaged, liquid fraction in packed beds. In pursuing this goal, the performance of ring electrodes in pipes containing gas–liquid mixtures is also carefully evaluated. Emphasis is given to studying the influence of geometrical electrode characteristics (mainly the separation distance between rings) for some typical gas–liquid distribution patterns. The latter comprise the cases of *segregated* (annular, stratified) and *uniformly distributed* gas–liquid mixtures.

In the following section, theory pertinent to the technique is briefly reviewed. A new analytical solution is also presented for predicting the ring electrode behavior in the case of an annular liquid distribution. In the next section, the experimental setup is outlined. A section follows on experimental results obtained under various conditions in a pipe and in a packed bed, and a comparison is made with theoretical predictions. An overall assessment of the technique is given in the final section.

THEORY

General Probe Characteristics

The use of flush mounted probes in two-phase systems is based on electrical potential field theory. Coney (1973) and Brown *et al.* (1978) provide theoretical treatments and performance analyses of such probes. As is well known, to suppress undesirable electrode polarization and capacitance effects, a sufficiently high frequency a.c. voltage excitation is applied; thus, the measured electrical impedance across an electrode pair is essentially resistive. The apparent conductance K_{app}, of a uniform liquid film of height h, covering a pair of electrodes of length δ, width S and separation distance D_e, is given (Coney 1973) by

$$K_{app} = K^*_{app}\, \delta\gamma, \qquad [1]$$

with

$$K^*_{app} = \frac{k(m)}{k(1-m)} \qquad [2]$$

and

$$m = \frac{\sinh^2\left(\dfrac{\pi S}{2h}\right)}{\sinh^2\left[\dfrac{\pi(S + D_e)}{2h}\right]}, \qquad$$

where K^*_{app} is a dimensionless conductance derived for two parallel strips of infinite length, embedded flush onto a *flat* surface, and γ is the liquid conductivity. The function k is the complete elliptic integral of the first kind (i.e. Abramowitz & Stegun 1964) and the parameter m is a function of the system geometry.

For circular electrodes covering an entire pipe circumference ($\delta = \pi D$) and for thin liquid films ($h \to 0$, $h \ll D_e$), [1] reduces to a simple approximate solution:

$$K_{app} = \frac{\pi D\gamma}{D_e}\, h. \qquad [3]$$

Hence, for very thin films the conductance between the ring electrodes is directly proportional to the product of the film height and the conductivity of the liquid. Experiments carried out by Asali et al. (1985) in annular films confirm this observation. Furthermore, Andreussi et al. (1988) showed that [3] holds even for thick asymmetric liquid layers, if simply the distance between the electrodes is sufficiently large with respect to the film height. An equivalent film height for this case is given as

$$h = \frac{A\beta}{\pi D}, \qquad [4]$$

where A is the pipe cross-sectional area and β is the volume fraction occupied by the liquid. To extend [3] to any separated liquid distribution pattern and to ducts of arbitrary cross-section, Andreussi et al. (1988) suggested the use of a generalized equivalent liquid height where πD is replaced by P_L, the duct wetted perimeter corresponding to a specific flow pattern.

To present and compare the experimental data with theory, it is advisable to normalize conductance measurements with the conductance of the pipe full of liquid, K_{max}. Thus, errors in the liquid conductivity measurements are eliminated. When packing is present the same equations hold. However, in normalizing the apparent probe conductance, one must take into account not only the full-pipe conductance but also the effective conductivity of the solid–liquid mixture, γ_e. The following normalized quantities are thus obtained:

annular without packing,

$$\frac{K_{app}}{K_{max}} = \frac{K_{app}^*}{K_{max}^*}; \qquad [5]$$

stratified without packing,

$$\frac{K_{app}}{K_{max}} = \frac{K_{app}^*}{K_{max}^*} \frac{\theta}{2\pi}; \qquad [6]$$

annular with packing,

$$\frac{K_{app}}{K_{max}} = \frac{K_{app}^*}{K_{max}^*} \frac{\gamma_e}{\gamma}; \qquad [7]$$

and

stratified with packing,

$$\frac{K_{app}}{K_{max}} = \frac{K_{app}^*}{K_{max}^*} \frac{\theta}{2\pi} \frac{\gamma_e}{\gamma}; \qquad [8]$$

where θ is the arc corresponding to the wetted perimeter.

The effective electrical conductivity γ_e, is a function of the continuous conducting phase (liquid) conductivity and the liquid volume fraction β. Solid particles and air are the dispersed substances. Of the numerous expressions proposed in the literature for computing γ_e, only the following are considered here:

Maxwell (1881),

$$\frac{\gamma_e}{\gamma} = \frac{2\beta}{3 - \beta}; \qquad [9]$$

Bruggeman (1935),

$$\frac{\gamma_e}{\gamma} = \beta^{3/2}; \qquad [10]$$

and

Begovich & Watson (1978),

$$\frac{\gamma_e}{\gamma} = \beta. \qquad [11]$$

If the liquid phase is *uniformly distributed* throughout the packing, the normalized conductance is obviously equal to the relative conductivity; i.e.

$$\frac{(K_{app})_{dis}}{K_{max}} = \frac{\gamma_e}{\gamma}.$$
[12]

Therefore, it is expected that, in the case of a uniformly distributed liquid, the ratio $(K_{app})_{dis}/K_{max}$ will be dependent only on the liquid fraction β and independent of the ring probe geometric characteristics (S, D_e).

Analysis of the Probe Response to a Conducting Annulus

The geometry considered is depicted in figure 1, where due to cylindrical symmetry only a cross-section is drawn. The problem is described by the Laplace equation for the electric potential V, with the appropriate boundary conditions:

$$\nabla^2 V = 0$$
[13]

$$\frac{\partial V}{\partial r'} = 0, \qquad r' = r;$$
[14]

$$\frac{\partial V}{\partial r'} = 0, \qquad r' = R, \quad -c_1 < z' < -\lambda, \quad -1 < z' < 1, \quad \lambda < z' < c_2;$$
[15]

$$\frac{\partial V}{\partial z'} = 0, \qquad z' = -c_1, \quad z' = c_2;$$
[16]

$$V = V_0, \qquad r' = R, \qquad 1 < z' < \lambda;$$
[17]

and

$$V = -V_0, \quad r' = R, \quad -\lambda < z' < -1;$$
[18]

where V_0 is the electric potential on the probe surface, r is the inner and R the outer radius of the annulus; c_1, c_2 denote the location of the circular bounding surfaces and λ is defined in figure 1. All lengths are made dimensionless with respect to $(D_e - S)/2$. A dimensionless conductance is defined as follows:

$$K_{app}^* = -\frac{1}{V_0} \int_1^\lambda \left(\frac{\partial V}{\partial r'}\right)_R dz' = \frac{2K_{app}}{2\pi R\gamma(D_e - S)}.$$
[19]

This problem is difficult to tackle (even by numerical methods) due to the discontinuities of the boundary conditions on the surface $r' = R$. To obtain a physically meaningful analytic solution, it is assumed that for electrodes of relatively small width the distribution of current density on their
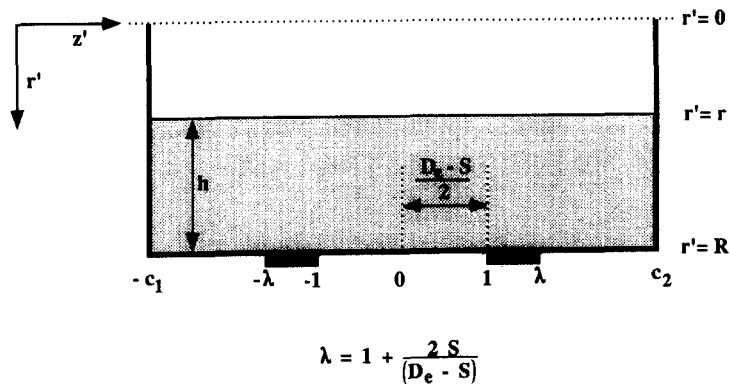

$$\lambda = 1 + \frac{2\,S}{(D_e - S)}$$

Figure 1. Geometrical arrangement of two ring electrodes in contact with a conducting annulus of finite thickness, $h = R - r$.

surface is *uniform*. Thus, the original "mixed"-type problem is changed to a Neumann problem, where boundary conditions [17] and [18] are substituted by

$$-\frac{2\gamma}{D_e - S}\frac{\partial V}{\partial r'} = Q, \qquad r' = R, \qquad 1 < z' < \lambda;$$ [20]

and

$$-\frac{2\gamma}{D_e - S}\frac{\partial V}{\partial r'} = -Q, \qquad r' = R, \qquad -\lambda < z' < -1.$$ [21]

Here Q is the current density. The conductance is now given as

$$K^*_{app} = \frac{Q(D_e - S)(\lambda - 1)^2}{2\gamma}\left(\int_1^\lambda V\,dz'\right)^{-1}.$$ [22]

The following analytic solution to the above problem is obtained by the method of separation of variables:

$$K^*_{app} = \frac{\pi^3}{2}\left(\frac{\lambda - 1}{c_1 + c_2}\right)^2\left(\sum_{i=1}^\infty \frac{1}{i^3} a_i^2 f_i\right)^{-1},$$ [23]

with

$$a_i = \sin[\kappa_i(c_1 + \lambda)] - \sin[\kappa_i(c_1 + 1)] - \sin[\kappa_i(c_1 - 1)] + \sin[\kappa_i(c_1 - \lambda)]$$ [24]

and

$$f_i = \frac{I_0(\kappa_i R)}{I_1(\kappa_i R)}\left[\frac{1 + \dfrac{I_1(\kappa_i r)K_0(\kappa_i R)}{K_1(\kappa_i r)I_0(\kappa_i R)}}{1 - \dfrac{I_1(\kappa_i r)K_1(\kappa_i R)}{K_1(\kappa_i r)I_1(\kappa_i R)}}\right],$$ [25]

where I_0, K_0, I_1, K_1 are modified Bessel functions of the first and second kind (zero and first order) and the argument:

$$\kappa_i = \frac{i\pi}{c_1 + c_2}.$$

For the fully symmetric problem ($c_1 = c_2 = c$), the above solution is simpler:

$$K^*_{app} = \frac{\pi^3}{32}\left(\frac{\lambda - 1}{c}\right)^2\left[\sum_{i=0}^\infty \frac{1}{(2i + 1)^3} b_i^2 f_i\right]^{-1},$$ [26]

with

$$b_i = \cos(\hat{\kappa}_i\lambda) - \cos(\hat{\kappa}_i) \quad \text{and} \quad \hat{\kappa}_i = \frac{(2i + 1)\pi}{2c};$$

f_i is of the same form as in [25] with $\hat{\kappa}_i$ instead of κ_i.

To assess the validity of the assumed uniform current density distribution on the ring electrodes, the flat plate problem (two infinite strips, $c = \infty$) is solved under the same assumptions and the results are compared with the Coney (1973) solution. The flat plate solution is obtained from [26], where

$$f_i = \frac{1 + \exp(-2\hat{\kappa}_i h)}{1 - \exp(-2\hat{\kappa}_i h)}$$ [27]

and h is the liquid height. A comparison of the accurate Coney solution with the one obtained here reveals a relative error of $\sim 3\%$ and $\sim 2.5\%$, for $\lambda = 1.222$ and $\lambda = 1.105$, respectively, for $h = \infty$; however, this error tends to decrease with decreasing liquid height.

In general, the series solution [23] tends to underpredict somewhat the conductance with increasing λ. In the latter case the current density at the neighboring electrode edges tends to be greater than the average, thus deviating from the uniform distribution. A better approximation can be obtained by considering a *linear* current density distribution ρ, on each electrode, with $\rho = 0$ at the outer electrode edge:

$$\rho = \frac{2Q}{\lambda - 1}(\lambda - z').$$ [28]

The conductance for the symmetric problem is now given by [26] with $(b_i e_i)$ instead of $(b_i)^2$ and

$$e_i = \frac{2}{\lambda - 1}\left\{\lambda b_i + \frac{1}{\hat{\kappa}_i}[\sin(\hat{\kappa}_i\lambda) - \sin(\hat{\kappa}_i)]\right\}. \qquad [29]$$

Figure 2 shows that this is, indeed, a better approximation for electrodes of relatively large λ. The comparison in this figure corresponds to the most unfavorable liquid height ($h = \infty$).

Results similar to those depicted in figure 2 are obtained in the cylindrical geometry, where the linear current density distribution again provides a better approximation. However, for the relatively small values of the parameter λ which apply to our experimental system (and to most systems of practical interest), the uniform current density assumption leads to fairly accurate predictions. For this reason and due to its simplicity, a uniform current density is used in the following comparisons of the experimental data with theory.

EXPERIMENTAL SETUP AND PROCEDURES

The test section used in the experiments is a cylindrical column made of transparent Plexiglas. The column i.d. = 14 cm and length = 20 cm. The end plates are flanged to the cylinder. A schematic of the test section is shown in figure 3.

The packing material were fairly uniform glass spheres of 6 mm dia, giving an aspect ratio of $D/d_p = 23.3$ which is rather typical for packed beds. The column was packed layer by layer to make sure that the porosity of the bed was uniform. Each layer was packed by filling it with particles and applying uniform pressure at the top. The void fraction of the bed was determined to be 0.36 and the bed specific surface area to be 640 m^{-1}.

The liquid used in this work is tapwater, filtered mechanically to remove suspended particles larger than $5 \mu\text{m}$. Its specific conductivity varies between approx. 500 and 600 $\mu\text{S/cm}$. The observed scatter can be attributed, only in part, to room temperature fluctuations. However, by continuously monitoring conductivity and further reduction to a reference value, this problem is overcome.

Measurements are made by means of three parallel stainless steel ring electrodes, located 3 cm apart. The ring electrodes have a width of 3 mm. Two conductance probes may be formed: one comprised of two neighboring electrodes (3 cm apart) and the other by combining ring electrodes 6 cm apart. The electrodes are flush mounted onto the column wall to avoid disturbing the local porosity of the bed.

An a.c. carrier voltage of 25 kHz frequency is applied across each probe pair in order to eliminate capacitive impedance. Selection of the appropriate a.c. frequency value is made by measuring
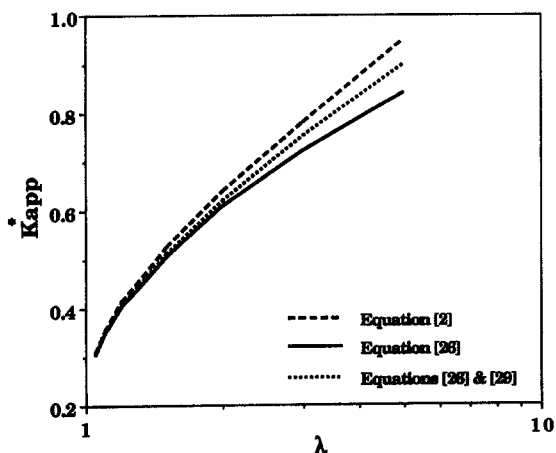

Figure 2. Comparison between solutions for different values of λ; flat plate geometry. The Coney (1973) solution [2] is compared with new solutions corresponding to a constant current density on each electrode [26] and to a linearly varying one [26] and [29].
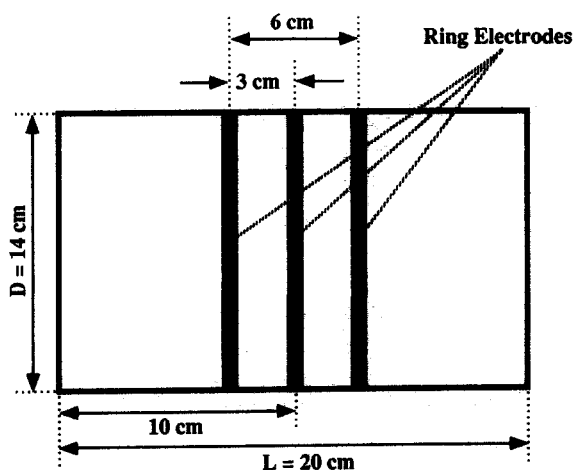
Figure 3. Electrode arrangement in the cylindrical test section; $z/L = 0$ designates the plane of symmetry.
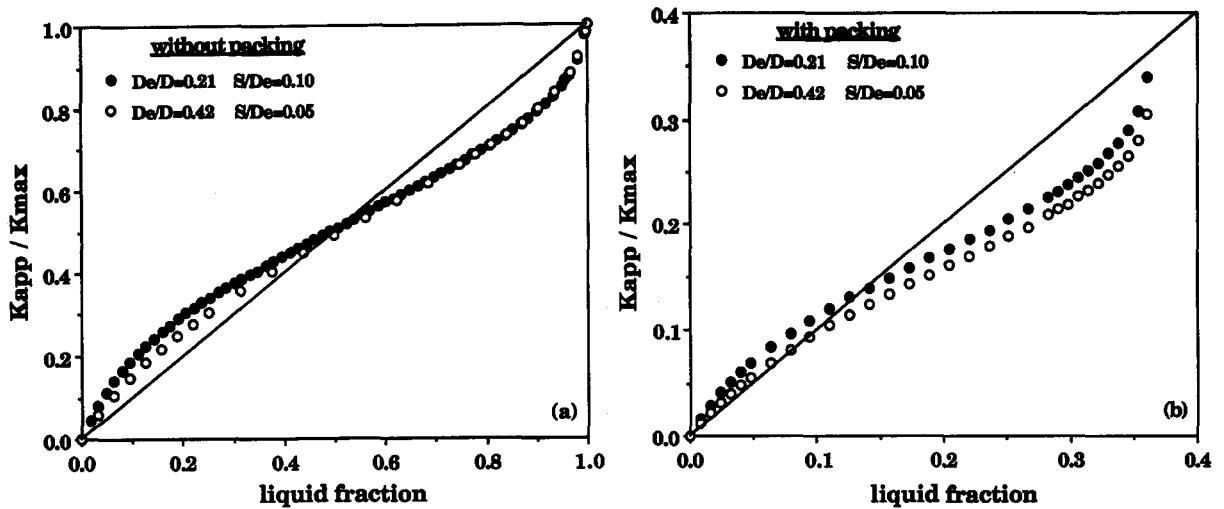
Figure 4. Dimensionless apparent conductivity vs liquid fraction for a stratified liquid distribution.

impedance magnitude and phase in the test section under various frequencies. An electronic signal analyzer converts the probe response to an analog output signal. The analyzer is similar to that employed by Karapantsios *et al.* (1989) and is characterized by high sensitivity and stability. Testing and adjustment of the analyzer is necessary before each set of measurements by using precision resistors.

The analog signal from each probe is uniquely related to the conductance of the medium between the electrodes. Only one probe is used at a time, while the other is disconnected to avoid electronic interference. The analog signal from the analyzer is fed to a digital voltmeter and to an oscilloscope.

To achieve uniform liquid distribution, dynamic experiments are carried out in a trickle bed system. The column height in this system is 124 cm, while the column diameter and the packing material are the same as those of the above-mentioned test section. Tests are carried out under ambient conditions, with air and water flowing co-currently downwards. Water is sprayed uniformly on the top of the packing through a perforated distributor and air is introduced by means of another perforated tubular section. Water is supplied in the range 1.483–29.790 kg/m² s, while the gas flow rate is held constant at 0.055 kg/m² s. A long packed entrance section ensures adequate mixing of the two phases. The experimental setup for the dynamic experiments is described elsewhere (Tsochatzidis & Karabelas 1991).

Two probes are used in this case, of exactly the same fabrication, as outlined above, comprised of rings located 3 and 9 cm apart. The system is operated in the trickling flow regime (characterized by low gas and liquid flow rates) to avoid large liquid holdup and consequently conductance fluctuations. The dynamic liquid holdup is determined by the "quick-closing valves" technique. Fast responding electrically operated valves at the entrance and exit of the column are closed simultaneously and the trapped water is collected and weighed, while the signal from the conductance probe is recorded simultaneously.

RESULTS

Stratified Liquid Pattern

This liquid distribution pattern is obtained by introducing a known liquid volume into the cylindrical test section, lying horizontal. Figure 4(a, b) depicts data of K_{app}/K_{max} vs liquid fraction, taken with two probes of different geometry, for test sections *without* and *with* packing, respectively. An S-shaped curve is obtained in all cases, which is typical of the non-linear dependence of the apparent conductance on the liquid fraction. It will be pointed out here—as already discussed in the Theory section—that in figure 4(a, b), and in all other similar graphs, the conductance has been normalized with the maximum achievable conductance (K_{max}), i.e. that which corresponds to a test section with 100% liquid and no packing.
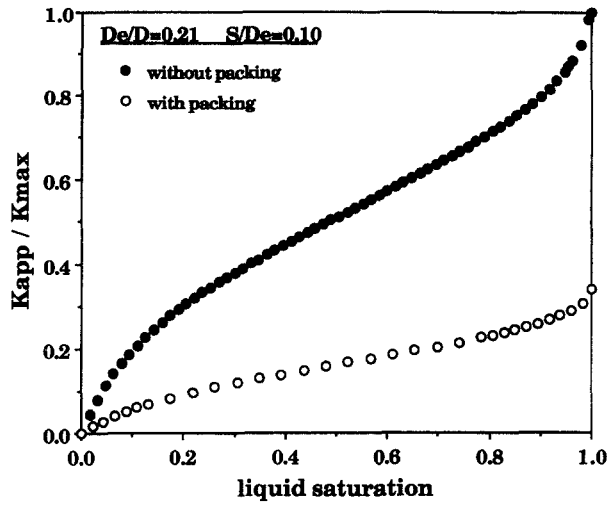
Figure 5. Comparison between data with closely spaced ring electrodes under stratified conditions, without and with packing.

For the case without packing, figure 4(a), the normalized conductance measured with the two (geometrically different) probes is practically identical for liquid fractions >0.5. This trend may be due to a good averaging of the probe signal, for such large volumes of liquid. For the case with packing, figure 4(b), the measurements taken with the two probes deviate systematically, which may be partly attributed to packing non-uniformity at the vessel wall, accentuated at small liquid fractions. The effect of such non-uniformities may be averaged out in the case of ring electrodes spaced relatively far apart.

In figure 5 a comparison is presented between measurements (with the same probe) without and with packing in the test section. The normalized conductivity is plotted vs "liquid saturation" LS, defined as

$$LS = \frac{\text{liquid volume}}{\text{bed volume} - \text{packing volume}}.$$

This coordinate is implicitly dependent on packing voidage. Moreover, there is a correspondence between LS and the equivalent liquid height inside the bed, thus allowing direct comparison of the conductance data for various bed void fractions. For example, LS = 0.5 corresponds to a half-full test section independent of packing voidage.
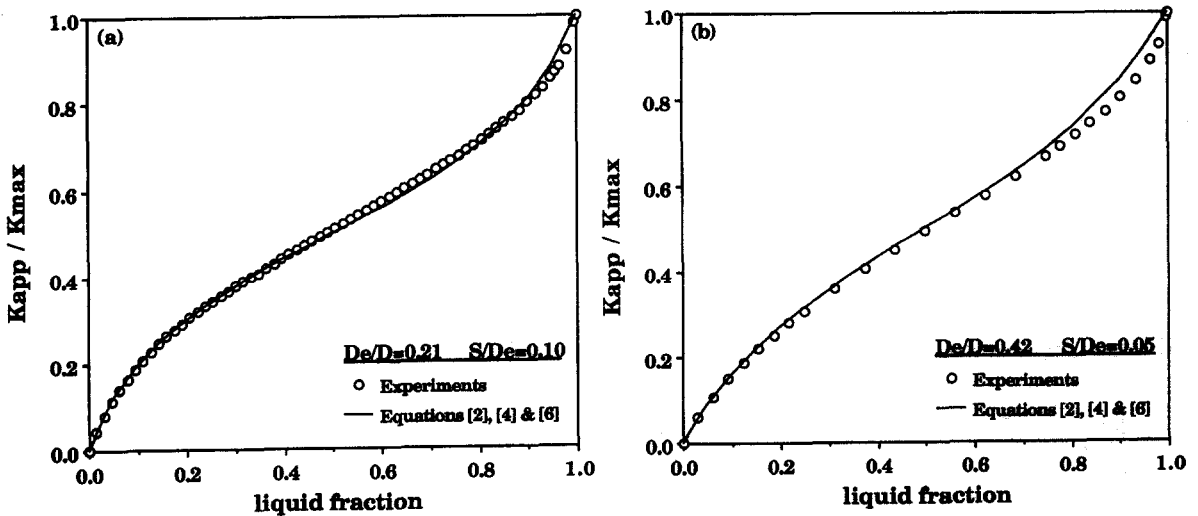

Figure 6. Comparison between theory and experiments under stratified conditions without packing; different electrode spacing. (a) $S/D_e = 0.10$; (b) $S/D_e = 0.05$.
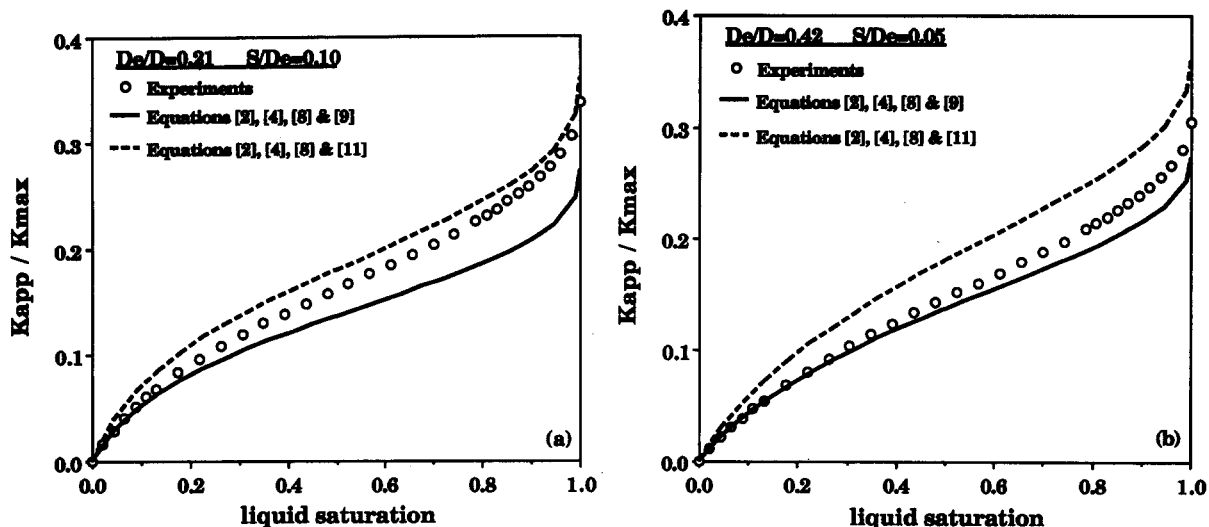
Figure 7. Comparison between theory and experiments under stratified conditions with packing and different electrode spacing.

The concept of an equivalent liquid layer, [4], will be assessed by comparing [6] with measurements. Figure 6(a, b) shows excellent overall agreement between data and predictions for the case of the test section *with no packing*. Only at liquid fractions approaching unity is there a discrepancy between data and computations. This may be attributed to the inadequacy of the theory when very thick liquid layers are involved. Nevertheless, the agreement is surprisingly good, especially if one considers that some experimental error may be involved, e.g. in specifying the precise geometrical probe characteristics.

In figure 7(a, b) a similar comparison is made between theory and data taken with two different probes in the section *with packing*. In both cases the normalized conductance falls between predictions based on Maxwell's [9] and on Begovich & Watson's [11] expressions for the effective electrical conductivity of the composite medium throughout the range of liquid fractions. At low liquid fractions, Maxwell's expression seems to perform better. However, it is difficult at present to recommend either one over the other. Moreover, recalling the uncertainty prevailing in the literature on the prediction of effective conductivity (in simpler geometries), one should be content with the fair agreement between the data and model predictions displayed by figure 7(a, b).
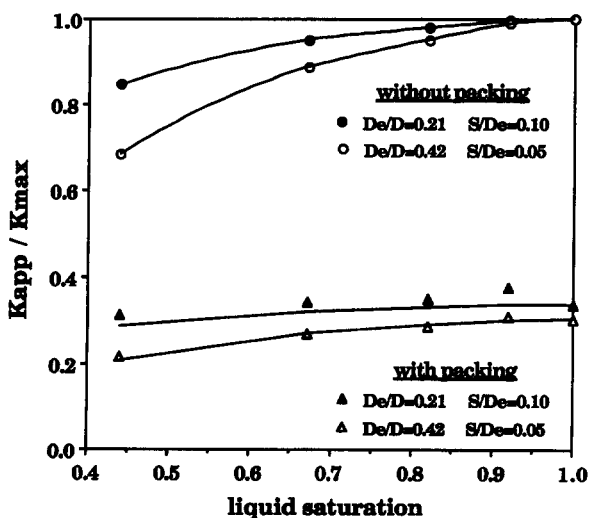

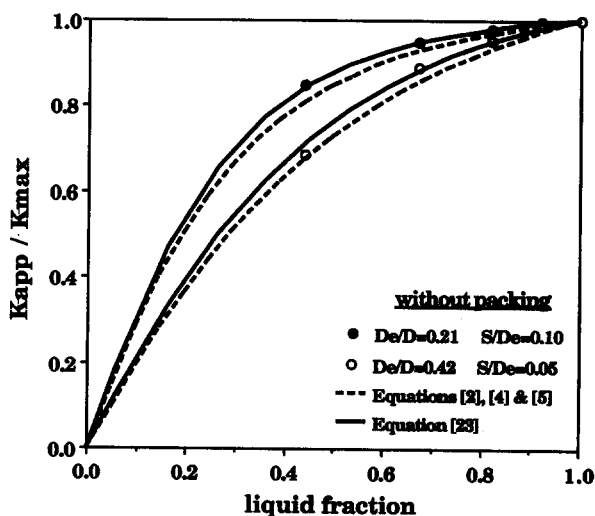Figure 8. Measurements taken with an annular liquid distribution.

Figure 9. Comparision between data for an annular liquid distribution without packing and theoretical predictions.

Annular Liquid Pattern

In static experiments this distribution pattern is simulated by placing solid Plexiglas rods of known diameter into the test section standing vertical. Experimental results for *symmetric* annular configurations are presented in figure 8, for a test section without and with packing. As expected, conductance tends to increase with increasing liquid fraction. The lines for the case without packing are the best fit through the data points. The lines for the case with packing are essentially those without packing, redrawn with the origin on the measured points at the maximum liquid fraction in the bed, i.e. 0.36. Experimental difficulties, to achieve uniformly close-packed conditions within the narrow annular gaps, is possibly the major cause of the discrepancy between estimates (solid line) and the data in the latter case. The data of figure 8 clearly show that, in the case of an annular liquid pattern, the sensitivity of closely spaced rings is inferior to that of rings spaced relatively far apart.

Figure 9 presents comparisons of the data with theoretical predictions, for a test section with no packing. The expression based on an equivalent liquid layer, [2], [4] and [5], provides estimates of K_{app}/K_{max} in fair agreement with measurements. On the other hand, it is shown that excellent agreement is obtained with [23] developed in this paper.

In the case of a test section with packing, figure 10 shows a comparison with predictions based on Maxwell's equation [9] and Begovich & Watson's equation [11] for effective conductivity. The former appears to fit better the data from electrodes placed 6 cm apart, and the latter data from electrodes 3 cm apart. However, no definitive statement can be made on the merits of either one of these expressions, in view of the possibility that the observed discrepancies (between the data and predictions) may be comparable to errors from non-uniform packing in the annulus.

Uniformly Distributed Liquid Pattern

Almost uniform liquid distribution is achieved by carrying out dynamic experiments in a trickle bed system, previously outlined. Trickling flow is usually considered to represent a uniform liquid distribution only when specific requirements are met. In particular, the bed aspect ratio must be >20 to minimize wall effects and a liquid distributor together with sufficient column height must be employed to avoid liquid maldistribution (Herskowitz & Smith 1983). These conditions are satisfied in our experimental system. Evidence to further support the development of a uniform distribution in our setup is given by Herskowitz & Smith (1978), who did experiments with a variety of packings and bed dimensions in the trickling flow regime. Specchia *et al.* (1974) also reported uniform flow in the trickling regime for a packed bed almost the same as ours (14.1 cm i.d. tube packed with glass beads 0.6 cm dia).
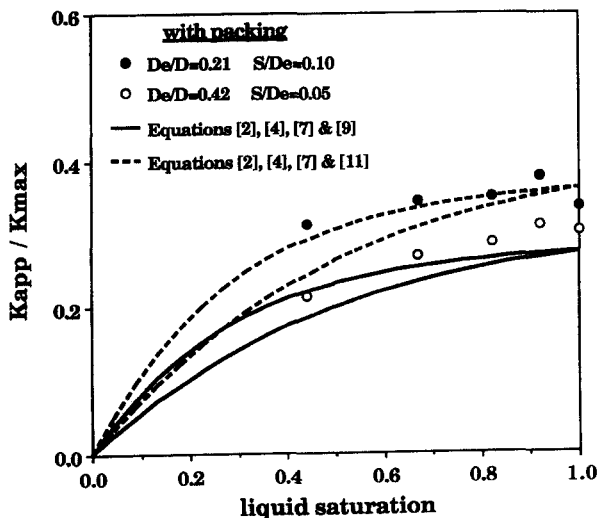

Figure 10. Comparison between predictions and data under an annular liquid distribution with packing.
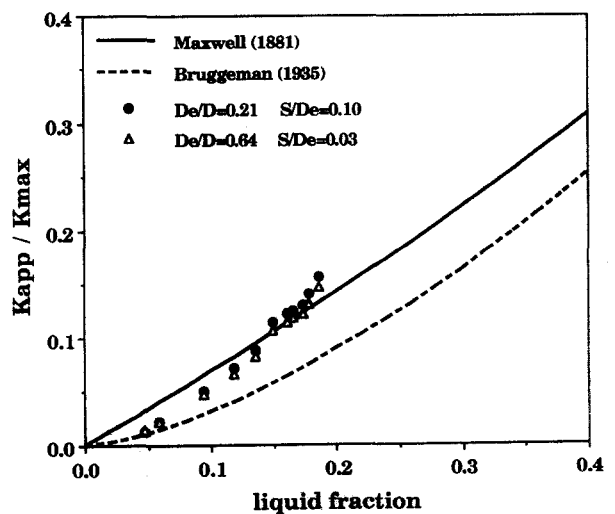
Figure 11. Comparison between predictions and data for a uniform liquid distribution.
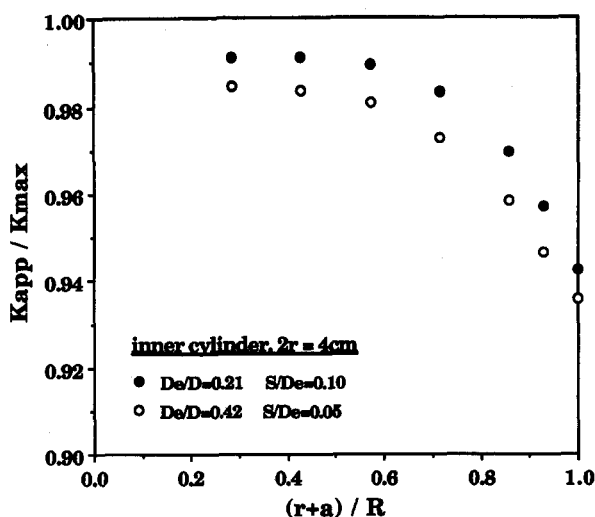
Figure 12. Radial response of the two probes for various annular liquid distributions without packing.
Data showing the effect of asymmetric annuli.

Experiments are performed with two probes characterized by $D_e = 3$ and 9 cm, in order to examine whether the normalized conductance, K_{app}/K_{max}, is indeed independent of the distance D_e between the ring electrodes, as indicated in the Theory section. Figure 11 shows that measurements made with both probes almost coincide, especially at small liquid fractions. Interestingly, the data fall along a curve which is roughly between similar curves based on Maxwell's (1881) and Bruggeman's (1935) expressions. Overall, neither of these expressions fits the measurements satisfactorily. For liquid fractions $> \sim 0.12$, Maxwell's relation is in fair agreement with the data. Bruggeman's expression appears to be satisfactory only at small liquid fractions; i.e. $< \sim 0.06$.

Sensitivity of the Experimental Technique

Radial non-uniformities

To assess the sensitivity of the probes to radial non-uniformities, Plexiglas rods of various diameters are placed in the test section parallel with its main axis. The probe response is recorded while moving the rod from the center toward the wall of the test section. These experiments are carried out with only liquid in the test section. No such measurements are made with packing, as it is difficult to achieve a uniform voidage in the asymmetric annular spaces generated by locating the rod at various distances from the wall. This problem is particularly acute in the case of narrow annular gaps.

Figure 12 depicts typical results of static experiments. The parameter a denotes the displacement of the center of the non-conducting rod from the center of the cross-section. The radius of the rod is r, so that a $\leqslant R - r$ and $(r + a)/R \leqslant 1.0$. In the case of an inner radius $r = 2$ cm (which corresponds to a liquid fraction of 0.92), the two probes display a similar response (figure 12), differing from the symmetric annulus ($a = 0$) value by at most $\sim 5\%$ when $a = R - r$. Other data, not presented here, show that for an inner radius with $r = 3$ cm and a liquid fraction of 0.82, the maximum difference of K_{app}/K_{max} from that of the symmetric annulus is $\sim 7\%$.

It must be noted at this point that Andreussi et al. (1988) report (for at least one probe of similar geometry—their figure 7) that no appreciable effect was observed as the Plexiglas rod moved to the wall, even for narrower annular gaps corresponding to liquid fractions <0.2. This does not appear to be in accord with the trend of our measurements. Nevertheless, it is felt that in most cases the errors due to asymmetric annuli (on a percentage basis) may be within the overall accuracy of the experiments.

It is pointed out here that the *angular response* of the probes does not warrant consideration due to the axial symmetry of the test section. This was verified experimentally (mainly to check the geometric accuracy of the experimental setup) by moving a non-conducting rod in the circumferential direction, at a fixed radial position.
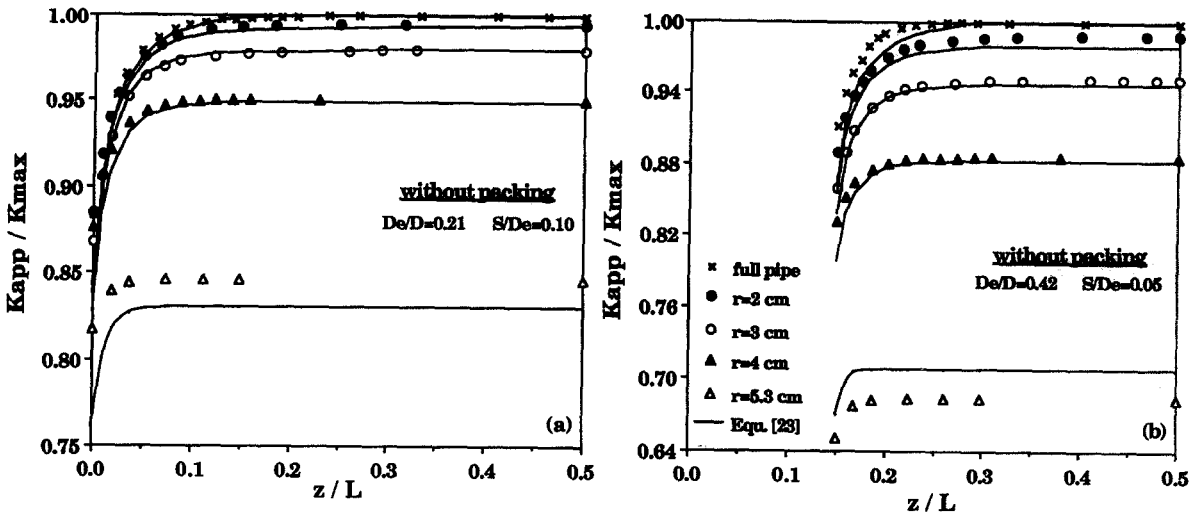
Figure 13. Axial response of the two probes for various annular distributions without packing. Non-conducting core of radius *r*. Comparison with predictions of the theory developed in this work.

Axial non-uniformities

The sensitivity of the probes to non-uniformities in the axial direction is quite important for practical applications. To assess such a sensitivity of flat parallel electrodes, Coney (1973) obtained computational results for a number of different probe geometries by assuming step-changes of film thickness in the axial direction.

The procedure employed in this work, to test for axial sensitivity, is to add known volumes of liquid into the test section (standing vertical), thus changing the gas–liquid interface position with respect to the probes. Figure 13(a, b) depicts relative conductance vs dimensionless distance from the plane of symmetry $z/L = 0$ of the test section (figure 3). The latter contains Plexiglas rods, creating symmetric annular liquid regions. A rather sharp increase is observed, to the nearly constant asymptotic value, which corresponds to probes well-covered (large z/L) with liquid. Furthermore, it is observed that electrodes spaced close together (e.g. $D_e/D = 0.21$) require slightly greater liquid coverage to reach the asymptotic value, as compared to electrodes spaced farther apart (e.g. $D_e/D = 0.42$). In general, it is noted that each electrode pair attains more than 90% of its asymptotic K_{app} value when the annular liquid layer just covers both ring electrodes; i.e. $z/L = 0$ for $D_e/D = 0.21$ and $z/L = 0.15$ for $D_e/D = 0.42$. The thinner the liquid layer the better the probe sensitivity, as is already known from the work of Asali *et al.* (1985).
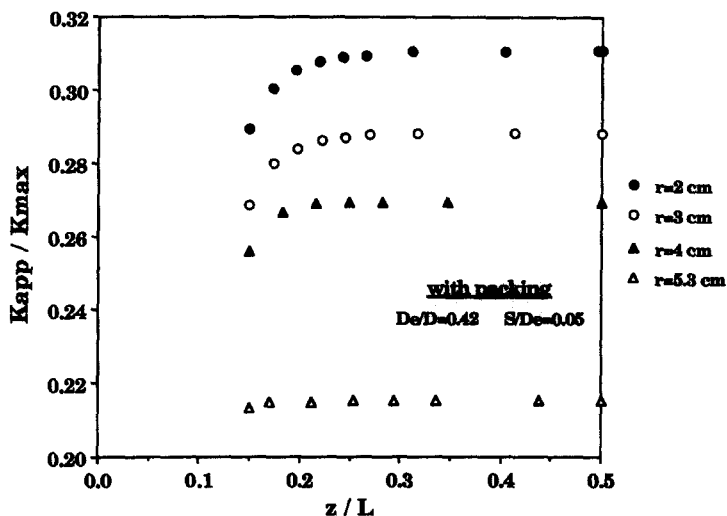

Figure 14. Axial response of one pair of electrodes for various annular distributions, with packing.
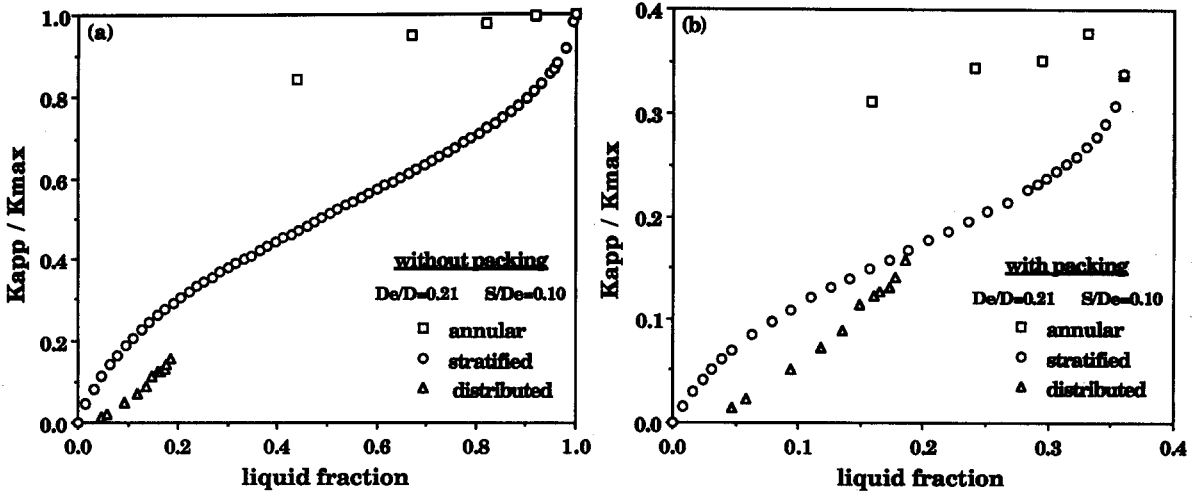
Figure 15. Response of closely spaced electrodes for various liquid distribution patterns, without and with packing.

Comparisons are made between measurements and predictions based on [23] developed here. The agreement is very satisfactory, especially if one considers the difficulties involved in specifying experimentally the exact location of the gas–liquid interface in the test section. Even for the worst case (a non-conducting cylinder with $r = 5.3$ cm) the discrepancy of $\sim 2\%$ falls within the accuracy of the measurements.

The same qualitative results are obtained with packing in the test section, as shown in figure 14. However, the inability to achieve a truly uniform packing porosity in the annular space leads to measured values which are systematically higher than predicted on the basis of either Maxwell's or Bruggeman's effective conductivity expressions.

DISCUSSION

The study of ring-type conductance probes presented here shows that the latter are robust and quite sensitive for making measurements of liquid holdup in two- and three-phase systems. The measured cross-sectionally averaged conductance as a function of liquid fraction (in packed beds and pipes) is influenced by the pattern of liquid distribution, i.e. stratified, annular and uniform, examined in this work. Qualitatively, measurements with gas–liquid mixtures in pipes and packed beds are very similar. The above trends are in agreement with predictions from existing theory and from a new analytical solution for annular liquid distributions presented here. Some discrepancies observed, when quantitative comparisons are made between predictions and data for packed beds, are attributed to the uncertainties about effective conductivity in three-phase media and to packing non-uniformities at the cylindrical surfaces.

Regarding potential practical applications, it is shown using data and theory that by proper selection of probe geometrical characteristics one can cope with various requirements, depending on the problem at hand. In particular, the technique is capable of discerning the aforementioned liquid distribution patterns (if the average liquid fraction is available), and of providing reliable cross-sectionally-averaged holdup data if the liquid pattern is known. However, in the latter case the use of calibration curves (obtained in static or dynamic type of tests) is required for precise holdup determination.

Figure 15(a, b) supports the above arguments, showing conductance measurements made with three different liquid distribution patterns, without and with packing in the test section. Figure 15(b) is perhaps of greater interest, suggesting that this technique may be employed for *non-intrusive* flow pattern recognition in packed beds.

The dual-ring probe displays satisfactory spatial sensitivity in the axial direction; i.e. the signal is influenced more than $\sim 90\%$ by the liquid distribution inside the cylindrical segment ("slice") bounded by the electrodes, as shown in figures 13(a, b) and 14(a, b). This probe feature (in agreement with theoretical predictions, [23]) is obviously significant for applications.

Finally, it will be noted that the technique is already used in this laboratory to study detailed characteristics of two-phase flow in packed beds, with very satisfactory results. In one application, pulsing flow in a trickle bed is studied in which the two-phase mixture is considered to be fairly evenly distributed in the radial direction (e.g. Herskowitz & Smith 1983), with periodic disturbances in the axial direction. For the uniformly distributed liquid case, it is shown in figure 11 that the ring electrode spacing does not influence the measurements. Therefore, to achieve satisfactory spatial resolution, experiments in the pulsing flow regime are carried out with closely spaced electrodes ($D_e = 3$ cm); i.e. with ring spacing shorter than the length of the disturbance being investigated. The response of this pair of electrodes to holdup fluctuations is very good, as shown elsewhere (Tsochatzidis & Karabelas 1991), permitting the acquisition of accurate data.

In another application, the liquid distribution in horizontal, axially rotated packed beds is studied (Karapantsios *et al.* 1991). Diagnosis of liquid distribution patterns is made possible with the dual-ring probe. Furthermore, rotation conditions leading to a nearly uniform liquid distribution are identified.

REFERENCES

ABRAMOWITZ, M. & STEGUN, I. A. 1964 *Handbook of Mathematical Functions.* Dover, New York.

ANDREUSSI, P. & BENDIKSEN, K. 1989. An investigation of void fraction in liquid slugs for horizontal and inclined gas–liquid pipe flow. *Int. J. Multiphase Flow* **15**, 937–946.

ANDREUSSI, P., DI DONFRANCESCO, A. & MESSIA, M. 1988 An impedance method for the measurement of liquid hold-up in two phase flow. *Int. J. Multiphase Flow* **14**, 777–785.

ASALI, J. C., HANRATTY, T. J. & ANDREUSSI, P. 1985 Interfacial drag and film height for vertical annular flow. *AIChE Jl* **31**, 895–902.

BECKMANN, H. & MEWES, D. 1991 Experimental studies of countercurrent flow in inclined tubes. Presented at the *Eur. Two-phase Flow Group Mtg*, Rome, paper B1.

BEGOVICH, J. M. & WATSON, J. S. 1978 An electroconductivity technique for the measurement of axial variation of holdups in three-phase fluidized beds. *AIChE Jl* **24**, 351–354.

BEIMESCH, W. E. & KESSLER, D. P., 1971 Liquid-gas distribution measurements in the pulsing regime of two-phase concurrent flow in packed beds. *AIChE Jl* **17**, 1160–1165.

BLOK, J. R. & DRINKENBURG, A. A. H. 1982 Hydrodynamic properties of pulses in two-phase downflow operated packed columns. *Chem. Engng J.* **25**, 89–99.

BLOK, J. R., VARKEVISSER, J. & DRINKENBURG, A. A. H. 1983 Transition to pulsing flow, holdup and pressure drop in packed columns with cocurrent gas–liquid downflow. *Chem. Engng Sci.* **38**, 687–699.

BROWN, R. C., ANDREUSSI, P. & ZANELLI, S. 1978 The use of wire probes for the measurement of liquid film thickness in annular gas–liquid flows. *Can. J. Chem. Engng* **56**, 754–757.

BRUGGEMAN, D. A. G. 1935 Calculation of different physical constants of heterogeneous substances. *Annln Phys.* **24**, 636–679.

CHASE, G. G., WILLIS, M. S. & KANNEL, J. 1990 Averaging volume size determination of electroconductive porosity probes. *Int. J. Multiphase Flow* **16**, 103–112.

CONEY, M. W. E. 1973 The theory and application of conductance probes for the measurement of liquid film thickness in two-phase flow. *J. Phys. E: Scient. Instrum.* **6**, 903–910.

DELHAYE, J. M., FAVREAU, C., SAIZ-JABARDO, J. M. & TOURNAIRE, A. 1987 Experimental investigation on the performance of impedance sensors with two and six electrodes for area-averaged void fraction measurements. In *ANS Proc. 1987 Natn Heat Transfer Conf.*, pp. 234–239.

HERSKOWITZ, M. & SMITH, J. M. 1978 Liquid distribution in trickle-bed reactors. *AIChE Jl* **24**, 439–450.

HERSKOWITZ, M. & SMITH, J. M. 1983 Trickle-bed reactors: a review. *AIChE Jl* **29**, 1–18.

HEWITT, G. F. 1978 *Measurement of Two Phase Flow Parameters.* Academic Press, London.

KARAPANTSIOS, T. D., PARAS, S. V. & KARABELAS, A. J. 1989 Statistical characteristics of free falling films at high Reynolds numbers. *Int. J. Multiphase Flow* **15**, 1–21.

KARAPANTSIOS, T. D., TSOCHATZIDIS, N. A. & KARABELAS, A. J. 1991 Liquid distribution in horizontal axially rotated packed beds. Presented at the *AIChE A. Mtg*, Los Angeles, CA, paper 202h.

MATUSZKIEWICZ, A., FLAMAND, J. C. & BOURÉ, J. A. 1987 The bubble-slug flow pattern transition and instabilities of void fraction waves. *Int. J. Multiphase Flow* **13**, 199–217.

MAXWELL, J. C. 1881 *A Treatise on Electricity and Magnetism*. Clarendon Press, Oxford.

MERILO, M., DECHENE, R. L. & CICHOWLAS, W. M. 1977 Void fraction measurement with a rotating electric field conductance gauge. *J. Heat Transfer* **99**, 330–332.

NASR-EL-DIN, H., SHOOK, C. A. & COLWELL, J. 1987 A conductivity probe for measuring local concentrations in slurry systems. *Int. J. Multiphase Flow* **13**, 365–378.

NYDAL, O. J. & ANDREUSSI, P. 1991 Gas entrainment in a long liquid slug advancing in a near horizontal pipe. *Int. J. Multiphase Flow* **17**, 179–189.

PROST, C. 1967 Etude des fluctuations de la texture du liquide s'écoulant a contre-courant ou a co-courant du gaz dans un garnissage de colonne d'absorption. *Chem. Engng Sci.* **22**, 1283–1297.

RAO, V. G. & DRINKENBURG, A. A. H. 1983 Pressure drop and hydrodynamic properties of pulses in two-phase gas–liquid downflow through packed columns. *Can. J. Chem. Engng* **61**, 158–167.

SAIZ-JABARDO, J. M. & BOURÉ, J. A. 1989 Experiments on void fraction waves. *Int. J. Multiphase Flow* **15**, 483–493.

SPECCHIA, V., ROSSINI, A. & BALDI, G. 1974 Distribution and radial spread of liquid in two-phase cocurrent flows in a packed bed. *Quad. Ing. Chim. Ital.* **10**, 171–182.

TSOCHATZIDIS, N. A. & KARABELAS, A. J. 1991 Hydrodynamic properties of pulses in trickle beds. In *Proc. 2nd Wld Conf. on Experimental Heat Transfer, Fluid Mechanics and Thermodynamics* (Edited by KEFFER, J. F., SHAH, R. K. & GANIC, E. N.), pp. 1515–1522. Elsevier, Amsterdam.

TURNER, J. C. R. 1976 Two-phase conductivity: the electrical conductance of liquid-fluidized beds of spheres. *Chem. Engng Sci.* **31**, 487–492.